Ecological Indicators 102 (2019) 746–751

Contents lists available at ScienceDirect

Ecological Indicators

journal homepage: www.elsevier.com/locate/ecolind

A novel index based on the cusp catastrophe theory for predicting harmful algae blooms

Yimei Tian[a], Bo Zheng[a,*], Hailiang Shen[b], Shengnan Zhang[a,c], Yaru Wang[d]

[a] School of Environmental Science and Engineering, Tianjin University, 135 Yaguan Road, Jinnan District, Tianjin 300350, China
[b] Computational Hydraulics International, 147 Wyndham St. N., Ste. 202, Guelph, Ontario, Canada
[c] Renai College, Tianjin University, Jinghai District, Tianjin 301636, China
[d] School of Electrical Engineering and Automation, Tianjin University, Nankai District, Tianjin 300072, China

ARTICLE INFO

Keywords:
Harmful algae blooms
Prediction
Cusp catastrophe
Drinking water safety

ABSTRACT

Harmful algae blooms (HABs) may occur in lakes and reservoirs, causing serious water quality problems. The occurrence of HABs is related to many water environmental indices. Hence, it is of great importance to develop new indices to predict HABs. In this study, a novel HABs prediction index named DCCPI (Discriminant of Cusp Catastrophe as the Prediction Index) was proposed based on the catastrophe theory. The DCCPI was calibrated and validated using a three-year dataset of observations of algae biomass, nutrients and environmental variables from the WS1 Reservoir in Northern China. The index was trained using the first two years and verified using the third year of observations. The index could accurately predict a HAB every year. The main advantage of this index is its ability to yield accurate predictions without the need for large training datasets. Thus, it can be especially suitable for areas with limited monitoring data. The DCCPI could serve as an effective tool for water managers to ensure the quality of water in lakes and reservoirs.

1. Introduction

Currently, most natural processes, either gradual or continuous, are accurately solved and modelled using calculus-based approaches (Tenreiro Machado et al., 2010; Machado et al., 2011). However, many phenomena, such as water boiling, ice melting, volcanic eruptions and harmful algae blooms (HABs) actually comprise abrupt temporal changes, or temporal discontinuities in otherwise continuous systems; therefore, using calculus to explore and model these systems is not considered appropriate(Henley, 1976; Chen and Chen, 2017). A HAB occurs as a result of specific nutrients and environmental conditions and causes serious ecological consequences (Maguire et al., 2016; Jauzein et al., 2018). In China, the consequences of HABs have long been reported(Jia et al., 2013; Xiao et al., 2017; Fang et al., 2018; Jauzein et al., 2018) and are of primary importance for human health, given that many cities are supplied with drinking water from reservoirs (Clark et al., 2017).

Many methods, models and equations have been applied so far to forecast HABs, such as Bayesian hierarchical models (Obenour et al., 2014), oceanographic models (Cusack et al., 2016; Dabrowski et al., 2016), evolutionary computation models (Recknagel et al., 2013), and artificial neural networks (ANNs). These linear and non-linear statistical models have limitations when the data involved are non-stationary (Cannas et al., 2006). The predictive accuracy of these methods (R^2 coefficient) may vary from 0.29 to 0.76 depending on the dataset used (Recknagel et al., 2013). ANNs have been widely applied in various research fields (Beyene, 2007; Raja et al., 2014), but they require increased computational capacity and their algorithm is optimized by minimizing training errors, often resulting in overfitting (Hagiwara and Fukumizu, 2008; Piotrowski and Napiorkowski, 2013). Thus, HABs may be predicted with low precision by some of these methods (Paerl and Otten, 2013; Dabrowski et al., 2016; Wang et al., 2017). Besides, it is often required to train a large dataset to reach accurate predictions. Due to the low socioeconomic level of some countries, there are currently many reservoirs and lakes that lack online monitoring systems. In these areas, monitoring is accomplished only by manual measurements and, because of the labor intensity, the monitoring frequency is low. As a result, it is very difficult to acquire large datasets that are essential for training ANNs. Thus, it is of great importance to introduce new theory and develop new indices that are effective with small amounts of data to improve the predictive accuracy of HABs prediction.

The catastrophe theory can handle complex linear and nonlinear relationships simultaneously, using a high order probability density

* Corresponding author.
E-mail address: yejustme@tju.edu.cn (B. Zheng).

https://doi.org/10.1016/j.ecolind.2019.03.044
Received 12 November 2018; Received in revised form 20 March 2019; Accepted 22 March 2019
Available online 28 March 2019
1470-160X/ © 2019 Elsevier Ltd. All rights reserved.

function that has the advantage of being able to incorporate sudden behavioral jumps (Zeeman, 1976; Wagenmakers et al., 2005). It is particularly suitable for systems in which continuous changes of parameters can result in discontinuous changes in outcome variables (Chow et al., 2015). Historically, it has been widely used in social and behavioral sciences (Chow et al., 2015), for example, for analyzing sudden changes in a person's behavior (Hu and Xia, 2015), crowd congestion in public buildings (Zheng et al., 2010), traffic(Papacharalampous and Vlahogianni, 2014), efficient word reading (Sideridis et al., 2016) and public health (Chen and Chen, 2017). However, the cusp catastrophe model has seldom been reported in the fields of natural sciences and engineering, especially in the fields of HABs prediction (Petraitis and Dudgeon, 2016; Townhill et al., 2018).

The goal of this article is to provide an overview of the cusp catastrophe model, focusing on its application in the prediction of HABs. In this study, we developed a novel index, the DCCPI (Discriminant of Cusp Catastrophe as the Prediction Index) based on the cusp catastrophe theory, to predict the occurrence of a HAB at a given date, using the values of specific nutrients and environmental variables of the previous available date, which were selected from an initial pool of candidate variables. The primary advantage of this index, compared to other available indices and methods, is its ability to provide HAB predictions even with the use of small datasets. The index was developed and validated using a three-year monitoring dataset from the WS1 Reservoir in Northern China.

2. Materials and methods

2.1. Overview of the cusp catastrophe theory

Within specific limitations, catastrophic natural phenomena, those that undergo periods of sudden changes and reversals, can be classified in seven elementary catastrophes, the cusp catastrophe being one of them (Rene, 1975). A fundamental concept in the cusp catastrophe theory is the system's 'potential', its tendency towards the occurrence of a specific sudden outcome. Catastrophic phenomena undergo periods of equilibrium, where the potential is minimum, and periods of sudden changes, where the potential is maximum. The system's potential is not a structurally stable function but has a degenerate critical point (singularity). In the cusp catastrophe theory, stability is accomplished by using three variables to stabilize the degenerate critical point, within the following equation (Chen et al., 2014; Papacharalampous and Vlahogianni, 2014)

$$V(x) = x^4 + ux^2 + vx \tag{1}$$

where V is the system's potential, x is the state variable, and u and v are the control variables (normal variable and splitting variable, respectively). The normal variable determines when the sudden jump will occur and the splitting variable regulates the scale of the jump. By taking the derivative of Eq. (1), the equilibrium surface can be obtained (Chen et al., 2014), as shown in Eq. (2) and Fig. 1. In Fig. 1, the surface consists of two stable regions and a folded area. The folded area can be projected to the bifurcation set. The boundary of the bifurcation set satisfies Eq. (4) which is deduced by eliminating x through connecting Eqs. (2) and (3).

$$\frac{dV(x)}{dx} = 4x^3 + 2ux + v = 0 \tag{2}$$

$$\frac{d^2V(x)}{dx^2} = 12x^2 + 2u = 0 \tag{3}$$

$$8u^3 + 27v^2 = 0 \tag{4}$$

$$\Delta = 8u^3 + 27v^2 \tag{5}$$

When (u, v) is outside the bifurcation set, changes in the control variables will lead only to a continual change in the system status.

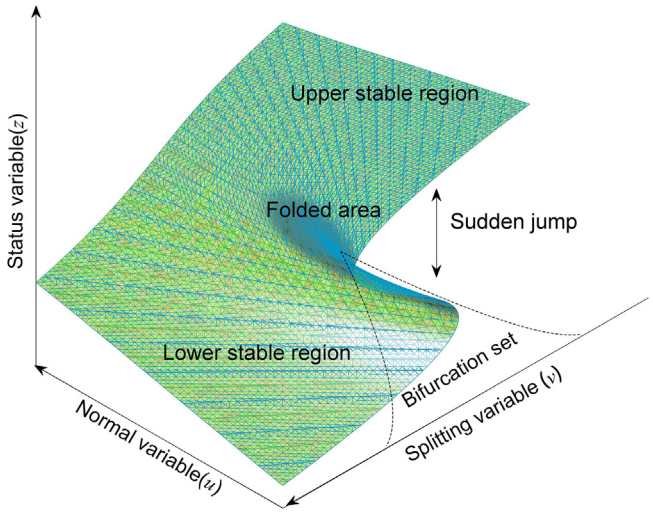

Fig. 1. Equilibrium surface of cusp catastrophe. The equilibrium surface can be divided into two stable regions (the upper and lower stable region) and a unstable region. The folded area can be projected to the bifurcation set. When the point (u, v) enters the bifurcation set, a sudden jump of the state variable will occur and cause a catastrophe of the system.

However, when the point enters the bifurcation set, a sudden jump of the state variable occurs. Since the boundary of the bifurcation set satisfies Eq. (4), the discriminant is defined as in Eq. (5). According to this theory, when the discriminant decreases sharply to a small negative value, cusp catastrophe will occur.

2.2. The components of DCCPI

It is essential to select proper components as the control variables and state variable. The algae cell density was selected as the state variable.

The occurrence of HABs has been associated with excessive increases in the values of phosphorus (P) and nitrogen (N) (Conley et al., 2009). It is considered that if the N:P ratio is ≥ 30:1, P is the limiting factor, and when N:P ≤ 5:1, the limiting factor is N (Havens et al., 2003; Huang et al., 2016). Moreover, since HABs are actually regarded as the outcome of a specific combination of nutrients and environmental factors, total P, total N, ammonia-nitrogen (NH_3-N) and nitrate-nitrogen (NO_3-N) were considered as candidates for normal variables, while temperature, pH, alkalinity and turbidity were considered as candidates for splitting variables. But as both the control and splitting variables have to be unique, a Principal Components Analysis (PCA) was applied for the normal variables to find those interrelated and select the one with the highest degree of influence on the response variable. The splitting variables were combined in one by using a specific equation formulated according to expert judgment. All these data are shown in Table S1.

2.3. Constructing the DCCPI

In order to eliminate the influence of dimension, all variables were normalized based on the following equation:

$$x'_{ij} = \frac{(x_{ij} - x_{j\min})}{(x_{j\max} - x_{j\min})} \tag{6}$$

where x_{ij}'denotes the normalized value of the j-th variable at time i, $x_{ij}$is the actual value of the j-th variable at time i, x_{jmin} denotes the minimum value of the j-th variable for the whole time period and x_{jmax} denotes the maximum value of the j-th variable for the whole time period. Eq. (2) is transformed to

$$4x^3 = -2ux - v \quad (7)$$

Let $y = 4x^3$, $u = k_1u'$, $v = k_2v' - k_3$. Then, from Eq. (7) we get:

$$y = k_1(-2u'x) + k_2(-v') + k_3 \quad (8)$$

where x is the normalized state variable, u' and v' are the normalized values of the normal and splitting variables, respectively. Then, Eq. (8) is converted into the following matrix:

$$Y = XB$$

$$X = \begin{bmatrix} -2u_1'x_1 & -v_1' & 1 \\ -2u_2'x_2 & -v_2' & 1 \\ \vdots & \vdots & \vdots \\ -2u_n'x_n & -v_n' & 1 \end{bmatrix}$$

$$B = [k_1 \quad k_2 \quad k_3]^T \quad (9)$$

where n is the number of samples. Vector B can be solved by the multiple regression method.

Instead of modelling x (the normalized algae-cell density) in Eq. (8), we solve for $y = 4x^3$, which can be simulated by the right side of Eq. (8). Thus, the DCCPI is the discriminant of Eq. (8), which based on Eq. (4), it is the following:

$$\mathrm{DCCPI} = 8(k_1u')^3 + 27(k_2v' - k_3)^2 \quad (10)$$

2.4. Solving the parameters of DCCPI

We used a three-year dataset of regular observations of algae-cell density (Fig. 2) and various nutrients and environmental variables (Table S1). In order to predict the occurrence of a HAB at a specific day, the DCCPI needs to be calculated from the values of the previous day available. For example, to predict the state variable x (algae-cell density) on August 23, the DCCPI for August 23 needs to be calculated-predicted from the u and v values of August 15 (the previous day available). Significant changes in the DCCPI values between consecutive dates would suggest the occurrence of a HAB.

For solving the DCCPI parameters, we tested the predictive accuracy of two alternatives, (i) the use of both total N and total P as components of the normal variable (DCV option) and (ii) the use only of total P as the normal variable (TP-CV option), since in our dataset, the N:P ratio was ≥30:1 for 73% of the time period studied. The first two years of records were used for the development of the DCCPI and the records of the third year were used for validation. The Pearson correlation coefficient R between the observed and fitted value was calculated. We finally selected the option with the highest predictive accuracy (highest R value) as the final DCCPI.

Besides the WS1 Reservoir, we have monitored another nitrogen-rich water reservoir (WS2, datasets in Table S2) for one year. These two options were also used for solving the DCCPI parameters of the WS2 Reservoir.

Table 1
Results of the Principal Components Analysis for the nutrients factors.

Variable	Factor loading			
	PC1[1]	PC2	PC3	PC4
TP	−0.5068	−0.1771	0.8429	0.0355
TN	0.6108	0.0006	0.3371	0.7164
NH_3-N	−0.0611	0.9829	0.171	−0.0291
NO_3-N	0.6053	−0.0496	0.3828	−0.6961
Eigenvalue	2.4579	1.0111	0.4742	0.0568
(%)	61.4	25.3	11.9	1.4

[1] For Tables 1 and 2, 'PC1' is the abbreviation of 'principal components 1'. PC2, PC3, and PC4 are similar.

Table 2
Results of the Principal Components Analysis for the environmental factors.

Variable	Factor loading			
	PC1	PC2	PC3	PC4
Temperature	−0.5246	−0.5085	−0.2793	0.623
pH	−0.3954	0.8507	−0.2318	0.2574
Alkalinity	0.5789	0.1325	0.319	0.7386
Turbidity	−0.483	0.0147	0.8755	−0.0022
Eigenvalue	2.6053	0.7708	0.5114	0.1125
(%)	65.1	19.3	12.8	2.8

3. Results and discussion

The results of the PCA analysis for the normalized values of the candidate variables are shown in Tables 1 and 2.

The first two principal components of each analysis were chosen as the components of the normal variable and splitting variable based on their cumulative percent contribution rates (86.7% and 84.4%) respectively. Because the cusp catastrophe theory can only accept a single variable as its normal variable or splitting variable, no matter how many principal components we select, we have to combine them into one single variable. The combination method is adding all the selected principal components together. For the DCV option, the normalized normal variable is

$$u' = -0.6839u_1' + 0.6114u_2' + 0.9218u_3' + 0.5557u_4' \quad (11)$$

where u_1', u_2', u_3', u_4' are the normalized value of TP, TN, NH_3-N and NO_3-N, respectively. The normalized splitting variable is

$$v' = -1.0331v_1' + 0.4553v_2' + 0.7114v_3' - 0.4683v_4' \quad (12)$$

where v_1', v_2', v_3', v_4' are the normalized values of temperature, pH,

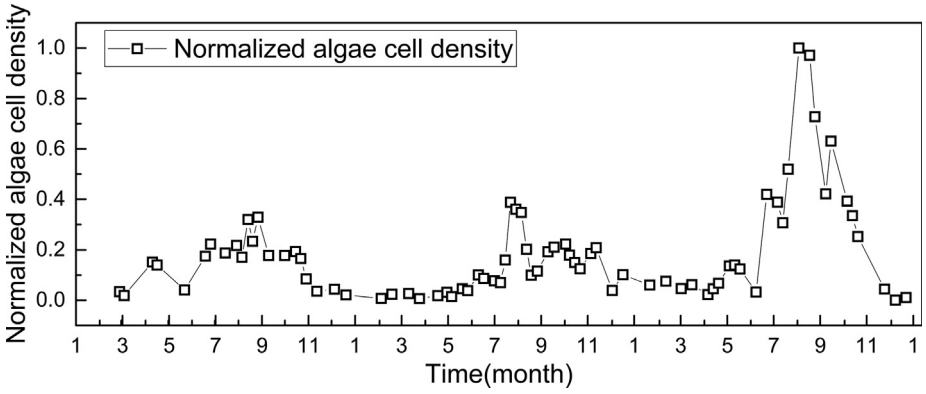

Fig. 2. Normalized value of algae cell density of the WS1 Reservoir. In every summer, a HAB occurred when the algae cell density increased sharply.

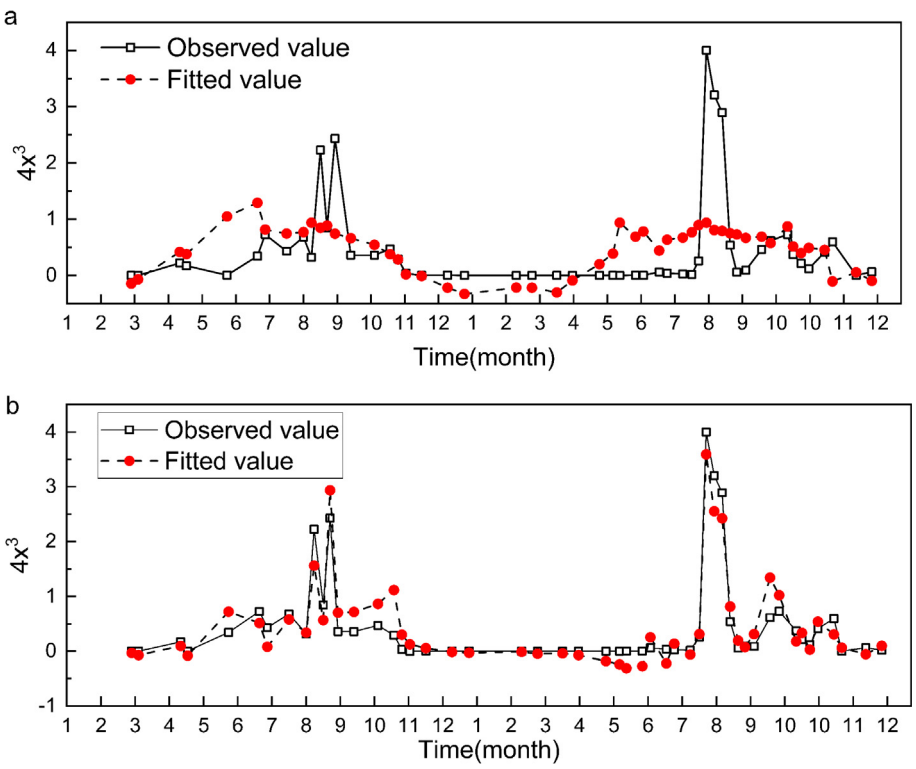

Fig. 3. Observed and fitted $4x^3$ values (x denotes the 0–1 normalized algae cell density) of the two DCCPI options. (a) DCV option:TP, TN, NH_3-N, and NO_3-N were selected as the components of the normal variable, while temperature, pH, alkalinity, and turbidity were selected as the components of the splitting variable. (b) TP-CV option: only TP were selected as the components of the normal variable, while the splitting variable was the same as that of the DCV option.

alkalinity, and turbidity, respectively.

For the TP-CV option, TP was used as the normalized normal variable, while the normalized splitting variable was the same as in Eq. (12).

3.1. Predictive capacity of the various DCCPI options

The TP-CV option was highly accurate (R = 0.941) in predicting HAB occurrences (Fig. 3b), in contrast to the DCV option, which had low predictive performance (R = 0.484) (Fig. 3a).

In this reservoir, phosphorus is the limiting factor (N:P ≥ 30:1 for 73% of the time period studied). Due to the high nitrogen concentration, the variation of phosphorus is the mainly limited factor of HABs. Because of the richness of nitrogen, the variation of nitrogen-related indices had little correlation with the occurrence of HABs. Therefore, using TN, NH_3-N and NO_3-N as components of the normal variable would disturb the cusp catastrophe and result in bad fitting precision.

Using the TP-CV option, a HAB can be predicted by DCCPI in every summer (Fig. 4). In the first year, the DCCPI value calculated by the data of August 29 dramatically decreased to a minimum value −56.2, and the observed value reached 2.43 on September 5, during the HAB. A similar trend was observed for the second year, with a DCCPI minimum at −50 before the occurrence of the HAB. In addition, the DCCPI could warn of medium increases of algae biomass in other seasons.

Based on our dataset, the solved k_i values were

$$k_1 = -1.9586,\quad k_2 = -0.3610,\ k_3 = -0.3914 \tag{13}$$

and the final DCCPI was

$$\mathrm{DCCPI} = -60.1073u'^3 + 27(-0.3610v' + 0.3914)^2 \tag{14}$$

where u' is the normalized value of total phosphorus and v' is the combined variable of temperature, pH, alkalinity, and turbidity, as in Eq. (12).

3.2. Validation of the DCCPI

The DCPPI equation was verified using the monitoring data of the third year, showing high accuracy (R = 0.873) (Fig. 5). The correlation coefficient R for the predictions of the DCCPI for the third year of our

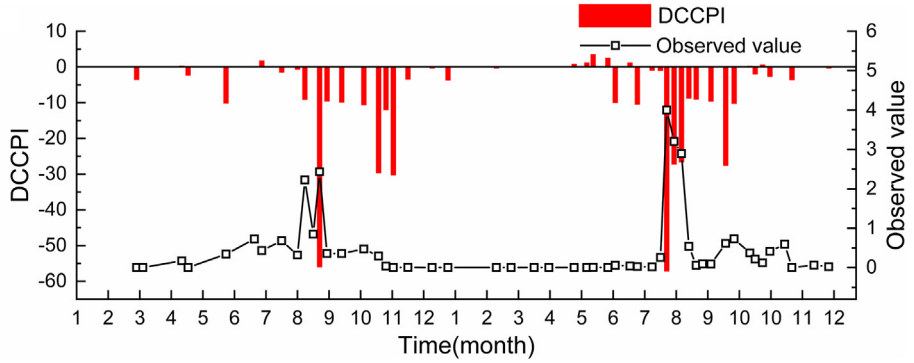

Fig. 4. Observed $4x^3$ values (x denotes the 0–1 normalized algae cell density) and DCCPI of the TP-CV option (only TP was selected as the component of the normal variable, while temperature, pH, alkalinity, and turbidity were selected as components of the splitting variable).

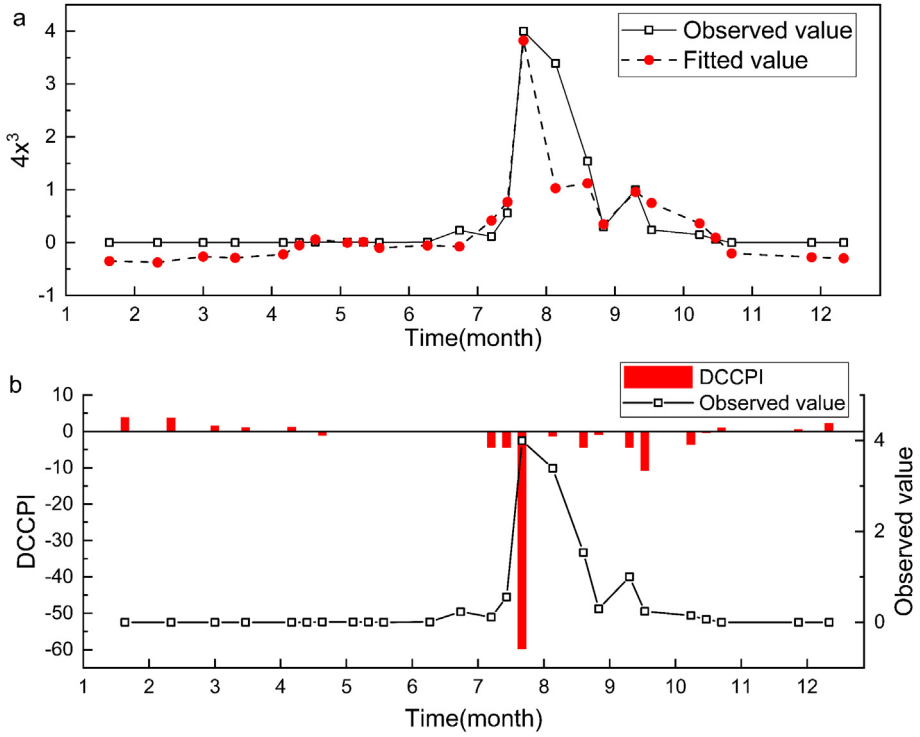

Fig. 5. Validation of the parameters of DCCPI with the data of the third year. (a) Observed and fitted $4x^3$ values (x denotes the 0–1 normalized algae cell density). (b) Observed $4x^3$ values (x denotes the 0–1 normalized algae cell density) and DCCPI of the TP-CV option.

dataset was 0.873 (Fig. 5). The DCCPI of the date of the HAB (July 29), calculated by the values of the previous available date (July 22) was < -50, suggesting the occurrence of the HAB in the near future. Then, a rapid increase of the DCCPI was evidenced in the next date.

For the WS2 reservoir, the TP-CV option could predict a HAB accurately as WS1 (Figs. S2 and S3). Hence, there are two examples to verify the TP-CV option of the nitrogen-rich waterbodies. As is shown by this study, for nitrogen-rich water bodies, only total phosphorus is necessary to be selected as the normal variable. Meanwhile, temperature, pH, alkalinity and turbidity should be selected as the splitting variable. Then, DCCPI calculated by the previous monitoring date can predict HABs effectively.

4. Conclusion

A novel HAB prediction index is proposed in this study. The accuracy of the DCCPI was evaluated using two options. The DCV option, including all nutrients in the prediction, failed to fit the observed value. The TP-CV option, with the only phosphorus as the normal variable and a combination of temperature, pH, alkalinity, and turbidity as the splitting variable, was highly accurate ($R = 0.943$). A three-year dataset was used for the DCCPI calibration and verification. The DCCPI was trained using data from the first two years and could accurately predict a HAB. There was a distinct difference between the normal DCCPI value (usually higher than -10) and critical DCCPI value (less than -50). The DCCPI was verified using the data of the third year. This index could be a useful tool to guarantee the supply of clean drinking water.

Acknowledgments

This work was supported by the Key Special Program of the S&T for the Pollution Control and Treatment of Water Bodies of China, China (grant number 2014ZX07203-009).

Competing interest statement

There is no any potential competing interest, including financial and non-financial, for each contributing author.

Appendix A. Supplementary data

Supplementary data to this article can be found online at https://doi.org/10.1016/j.ecolind.2019.03.044.

References

Beyene, W.W.T., 2007. Application of artificial neural networks to statistical analysis and nonlinear modeling of high-speed interconnect systems. IEEE Trans. Comput. Aided D 26 (1), 166–176.
Cannas, B., Fanni, A., See, L., Sias, G., 2006. Data preprocessing for river flow forecasting using neural networks: wavelet transforms and data partitioning. Phys. Chem. Earth 31 (18), 1164–1171.
Chen, D., Chen, X., 2017. Cusp catastrophe regression and its application in public health and behavioral research. Int. J. Environ. Res. Public Health 14 (12), 1220–1234.
Chen, D.D., Lin, F., Chen, X.J., Tang, W., Kitzman, H., 2014. Cusp catastrophe model. Nurs. Res. 63 (3), 211–220.
Chow, S., Witkiewitz, K., Grasman, R., Maisto, S.A., 2015. The cusp catastrophe model as cross-sectional and longitudinal mixture structural equation models. Psychol. Meth. 20 (1), 142–164.
Clark, J.M., Schaeffer, B.A., Darling, J.A., Urquhart, E.A., Johnston, J.M., Ignatius, A.R., Myer, M.H., Loftin, K.A., Werdell, P.J., Stumpf, R.P., 2017. Satellite monitoring of cyanobacterial harmful algal bloom frequency in recreational waters and drinking water sources. Ecol. Indic. 80, 84–95.
Conley, D.J., Paerl, H.W., Howarth, R.W., Boesch, D.F., Seitzinger, S.P., Havens, K.E., Lancelot, C., Likens, G.E., 2009. Ecology: controlling eutrophication: nitrogen and phosphorus. Science 323 (5917), 1014–1015.
Cusack, C., Dabrowski, T., Lyons, K., Berry, A., Westbrook, G., Salas, R., Duffy, C., Nolan, G., Silke, J., 2016. Harmful algal bloom forecast system for SW Ireland. Part II: are operational oceanographic models useful in a HAB warning system. Harmful Algae 53 (SI), 86–101.
Dabrowski, T., Lyons, K., Nolan, G., Berry, A., Cusack, C., Silke, J., 2016. Harmful algal bloom forecast system for SW Ireland. Part I: description and validation of an operational forecasting model. Harmful Algae 53 (SI), 64–76.
Fang, C., Song, K., Li, L., Wen, Z., Liu, G., Du, J., Shang, Y., Zhao, Y., 2018. Spatial variability and temporal dynamics of HABs in Northeast China. Ecol. Indic. 90, 280–294.
Hagiwara, K., Fukumizu, K., 2008. Relation between weight size and degree of over-

fitting in neural network regression. Neural Networks 21 (1), 48–58.
Havens, K.E., James, R.T., East, T.L., Smith, V.H., 2003. N: P ratios, light limitation, and cyanobacterial dominance in a subtropical lake impacted by non-point source nutrient pollution. Environ. Pollut. 122 (3), 379–390.
Henley, S., 1976. Catastrophe theory models in geology. J. Int. Assoc. Math. Geol. 8 (6), 649–655.
Hu, B., Xia, N., 2015. Cusp catastrophe model for sudden changes in a person's behavior. Inform. Sci. 294, 489–512.
Huang, S., Wu, M., Zang, C., Du, S., Domagalski, J., Gajewska, M., Gao, F., Lin, C., Guo, Y., Liu, B., Wang, S., Luo, Y., Szymkiewicz, A., Szymkiewicz, R., 2016. Dynamics of algae growth and nutrients in experimental enclosures culturing bighead carp and common carp: phosphorus dynamics. Int. J. Sediment Res. 31 (2), 173–180.
Jauzein, C., Acaf, L., Accoroni, S., Asnaghi, V., Fricke, A., Hachani, M.A., Saab, M.A., Chiantore, M., Mangialajo, L., Totti, C., Zaghmouri, I., Lemee, R., 2018. Optimization of sampling, cell collection and counting for the monitoring of benthic harmful algal blooms: application to Ostreopsis spp. blooms in the Mediterranean Sea. Ecol. Indic. 91, 116–127.
Jia, Y., Dan, J., Zhang, M., Kong, F., 2013. Growth characteristics of algae during early stages of phytoplankton bloom in Lake Taihu, China. J. Environ. Sci.-China 25 (2), 254–261.
Machado, J., Jesus, I.S., Barbosa, R., Silva, M., Reis, C., 2011. Application of fractional calculus in engineering. In: In: Peixoto, M.M., Pinto, A.A., Rand, D.A. (Eds.), Springer Proceedings in Mathematics, vol. 1. SPRINGER-VERLAG BERLIN, BERLIN, pp. 619–629.
Maguire, J., Cusack, C., Ruiz-Villarreal, M., Silke, J., McElligott, D., Davidson, K., 2016. Applied simulations and integrated modelling for the understanding of toxic and harmful algal blooms (ASIMUTH): integrated HAB forecast systems for Europe's Atlantic Arc. Harmful Algae 53 (SI), 160–166.
Obenour, D.R., Gronewold, A.D., Stow, C.A., Scavia, D., 2014. Using a Bayesian hierarchical model to improve Lake Erie cyanobacteria bloom forecasts. Water Resour. Res. 50 (10), 7847–7860.
Paerl, H.W., Otten, T.G., 2013. Harmful cyanobacterial blooms: causes, consequences, and controls. Microb. Ecol. 65 (4), 995–1010.
Papacharalampous, A.E., Vlahogianni, E.I., 2014. Modeling microscopic freeway traffic using cusp catastrophe theory. IEEE Intel. Transp. Syst. Mag. 6 (1), 6–16.
Petraitis, P.S., Dudgeon, S.R., 2016. Cusps and butterflies: multiple stable states in marine systems as catastrophes. Mar. Freshwater Res. 67 (1), 37–46.
Piotrowski, A.P., Napiorkowski, J.J., 2013. A comparison of methods to avoid overfitting in neural networks training in the case of catchment runoff modelling. J. Hydrol. 476 (11), 97–111.
Raja, M.A.Z., Samar, R., Rashidi, M.M., 2014. Application of three unsupervised neural network models to singular nonlinear BVP of transformed 2D Bratu equation. Neural Comput. Appl. 25 (7–8), 1585–1601.
Recknagel, F., Ostrovsky, I., Cao, H., Zohary, T., Zhang, X., 2013. Ecological relationships, thresholds and time-lags determining phytoplankton community dynamics of Lake Kinneret, Israel elucidated by evolutionary computation and wavelets. Ecol. Model. 255, 70–86.
Rene, T., 1975. Structural Stability and Morphogenesis: An Outline of a General Theory of Models. W.A.Benjamin, New York.
Sideridis, G.D., Simos, P., Mouzaki, A., Stamovlasis, D., 2016. Efficient word reading: automaticity of print-related skills indexed by rapid automatized naming through cusp-catastrophe modeling. Sci. Stud. Read. 20 (1), 6–19.
Tenreiro Machado, J.A., Silva, M.F., Barbosa, R.S., Jesus, I.S., Reis, C.M., Marcos, M.G., Galhano, A.F., 2010. Some applications of fractional calculus in engineering. Math. Prob. Eng. 2010 (639801), 1–34.
Townhill, B.L., Tinker, J., Jones, M., Pitois, S., Creach, V., Simpson, S.D., Dye, S., Bear, E., Pinnegar, J.K., 2018. Harmful algal blooms and climate change: exploring future distribution changes. ICES J. Mar. Sci. 75 (6), 1882–1893.
Wagenmakers, E.J., Molenaar, P., Grasman, R., Hartelman, P., van der Maas, H., 2005. Transformation invariant stochastic catastrophe theory. Phys. D 211 (3–4), 263–276.
Wang, L., Wang, X., Jin, X., Xu, J., Zhang, H., Yu, J., Sun, Q., Gao, C., Wang, L., 2017. Analysis of algae growth mechanism and water bloom prediction under the effect of multi-affecting factor. Saudi J. Biol. Sci. 24 (3), 556–562.
Xiao, X., He, J., Huang, H., Miller, T.R., Christakos, G., Reichwaldt, E.S., Ghadouani, A., Lin, S., Xu, X., Shi, J., 2017. A novel single-parameter approach for forecasting algal blooms. Water Res. 108, 222–231.
Zeeman, E.C., 1976. Catastrophe theory. Sci. Am. 234 (4), 65–83.
Zheng, X., Sun, J., Cheng, Y., 2010. Analysis of crowd jam in public buildings based on cusp-catastrophe theory. Build. Environ. 45 (8), 1755–1761.